Localized phonon-assisted cyclotron resonance in GaAs/AlAs quantum wells

J. S. Bhat
Department of Physics, Sri Dharmasthala Manjunatheshwara College of Engineering, Dharwad 580 002, India

B. G. Mulimani* and S. S. Kubakaddi
Department of Physics, Karnatak University, Dharwad 580 003, India
(Received 24 May 1993; revised manuscript received 10 February 1994)

The theory of phonon-assisted cyclotron resonance in quantum wells is given; we consider cases where electrons are scattered by confined LO phonons described by the Huang and Zhu model, Fuchs-Kliewer slab modes, and Ridley's guided mode model. The effect of interface phonon modes on cyclotron resonance is also studied. Extra peaks due to transitions between Landau levels accompanied by emission of confined and interface phonons in the absorption spectrum are predicted. Numerical results for frequency, field, and well-width dependence are given for parameters characteristic of GaAs/AlAs quantum wells.

I. INTRODUCTION

In recent years there has been much interest in the study of the effects of the electron-phonon interaction on the optical properties of two-dimensional electron systems formed in semiconductor heterojunctions and quantum wells (QW's) in the presence of a quantizing magnetic field.[1,2] In QW structures such as those formed from weakly polar III-V compound semiconducting materials, electron–polar-optical-phonon interaction plays a dominant role in determining various electronic properties. An important effect relevant to any discussion of electron-phonon interaction in the presence of a magnetic field is the phonon-assisted cyclotron resonance (PACR), in which electron transition between the Landau levels due to absorption of a photon is accompanied by absorption or emission of a phonon. There exist in the literature exhaustive theoretical[3–6] and experimental[7,8] investigations of PACR in bulk semiconductors. Calculations of PACR in two-dimensional QW structures[9–11] are based on a bulk description of the phonons. In widely studied QW structures such as GaAs/AlAs the optical-phonon branches of the two materials do not overlap, and hence an optical phonon in one material is heavily damped in the other. The optical phonons can therefore be considered to be confined to the individual layers. Also, the presence of heterointerfaces gives rise to interface modes which are localized in the vicinity of the interfaces. Raman spectroscopy measurements made upon superlattice (SL) structures,[12–14] and investigations[15–17] of I-V characteristics of phonon-assisted tunneling in $GaAs/Ga_{1-x}Al_xAs$ double-barrier resonant-tunneling structures, have confirmed the confinement of optical vibrations to the respective layers as well as the existence of interface modes.

Various models have been proposed to describe the confined and interface phonon modes. Of the two macroscopic dielectric continuum models, one corresponds to the "slab modes" of a free ionic slab[18,19] and the other to the "guided modes" of a model layered structure.[20] Recently, Huang and Zhu[21] (HZ) have proposed a simple lattice-dynamical model for describing phonon modes in SL's. These models differ in the way the boundary conditions are imposed on the electrostatic potential or vibrational amplitude of the phonons at the interfaces. Calculations of electron intra- and intersubband scattering rates in GaAs QW's due to confined LO phonons have been performed using the three models above, and estimates[22,23] based on the HZ model were found to be in good agreement with the experimental results.[24,25] Also, there have been theoretical investigations of electron scattering rates in QW's due to confined LO phonons, described by the above three models, in the presence of an applied electric field[26] and a quantizing magnetic field,[27] apart from the calculations of infrared absorption[28] and free-carrier absorption[29] based on the HZ model for confined phonons. The HZ model has received wide acceptance and best describes[30,31] the electron-phonon interaction in quasi-two-dimensional (Q2D) systems.

Various methods have been proposed to obtain interface modes in single or double heterostructures.[18,32–36] From an analysis of vibrational modes in an ionic slab, Fuchs and Kliewer[18] have found sinusoidal bulk LO modes with nodes at the interface and symmetrical and antisymmetrical interface modes which decay exponentially away from the interfaces. A Fröhlich-type Hamiltonian describing electron–optical-phonon interaction in a double heterostructure of a polar semiconductor was derived by Lassnig[32] using the electron energy loss method. Calculations of electron scattering rate[22] and infrared absorption[28] due to interface modes in GaAs/AlAs QW's, following the method of Lassnig, indicate that interface modes are as important as confined modes. Recent investigations of electron scattering rates due to interface optical phonons in GaAs/AlAs QW's (Ref. 37) and SL's (Ref. 38) in the presence of an electric field have indicated the strong coupling between electrons and interface modes.

To better understand electron-phonon interaction in QW's it is of interest to study PACR when electrons are

scattered by confined and interface optical phonons. Recently, Hai, Peeters, and Devreese[39] have studied the effects of interface and confined slab LO-phonon modes, described by a model due to Wendler and co-workers,[33,34] on polaron cyclotron resonance frequency for a GaAs/AlAs QW structure using memory-function formalism, and found that interface optical-phonon modes influence the magnetopolaron resonance considerably near the optical-phonon frequencies for narrow QW's. In this paper, following Bass and Levinson,[3] we present a theory of PACR in QW's employing a perturbation technique. This technique has been used successfully in analyzing PACR in bulk semiconductors and free-carrier absorption in low-dimensional structures.[40,41] One advantage of this method is its simplicity compared with the calculations based on linear response theory.[9,10,39] Our emphasis is on the HZ model. Calculations predict extra peaks in the magneto-optical spectrum due to transitions between Landau levels accompanied by absorption and emission of confined and interface optical phonons, besides the usual cyclotron resonance. Though the HZ model is well accepted[30,31] for describing the electron-phonon interaction in QW structures, for comparison, we present numerical results for confined modes described by the Fuchs-Kliewer slab modes, and Ridley's guided mode model. Also, we perform calculations to show the effect of electron interaction with interface optical-phonon modes on the PACR spectrum. In this we employ the model due to Lassnig.[32]

The paper is organized as follows. In Sec. II we outline the theory of electron-phonon interaction. In Sec. III we calculate absorption coefficients. We give the numerical results and discussion in Sec. IV.

II. ELECTRON-PHONON INTERACTION

A. Electron–confined-LO-phonon interaction

The electron–confined-LO-phonon interaction Hamiltonian as derived from the Fröhlich interaction is given by[19,21]

$$H_{\text{el-ph}}=\left[\frac{4\pi e^2\hbar\omega_{\text{LO}}}{V\varepsilon'}\right]^{1/2}\sum_{q,n}\sum_{\alpha=\pm}\exp(i\mathbf{q}\cdot\mathbf{r})t_{n\alpha}(q)u_{n\alpha}(z)\times[a_{n\alpha}(\mathbf{q})+a^{\dagger}_{n\alpha}(-\mathbf{q})]\ , \tag{1}$$

where $a,a^{\dagger}$ are the phonon annihilation and creation operators, $\varepsilon'=(\varepsilon_{\infty}^{-1}-\varepsilon_0^{-1})^{-1}$ with ε_0 and ε_{∞} denoting, respectively, the static and high-frequency dielectric constants, and V is the volume. $\mathbf{q}=(q_x,q_y)$ and $\mathbf{r}=(x,y)$ are, respectively, the two-dimensional phonon wave vector and the position vector in the plane of the layer and α are the even $(-)$ and odd $(+)$ confined phonon modes. $u_{n\alpha}(z)$ is the parallel component of the displacement vector in the direction of spatial confinement. For the HZ model[21] $u_{n\alpha}$ is given by

$$u_{n+}(z)=\sin\left[\frac{\mu_n\pi z}{L}\right]+\frac{C_n z}{L} \tag{2}$$

for odd modes, $n=3,5,7,\ldots$, and

$$u_{n-}(z)=\cos\left[\frac{n\pi z}{L}\right]-(-1)^{n/2} \tag{3}$$

for even modes, $n=2,4,6,\ldots$, with L denoting the width of the QW centered at $z=0$ and μ_n being solutions of

$$\tan(\mu_n\pi/2)=\mu_n\pi/2\ ,\quad n-1<\mu_n<n\ . \tag{4}$$

C_n are given by

$$C_n=-2\sin(\mu_n\pi/2)\ . \tag{5}$$

Note that odd modes start from $n=3$ in Eq. (2) as the $n=1$ mode corresponds to the interface modes.

The slab modes are obtained using the boundary conditions on the electric field without regard to the atomic displacements at the interfaces. The electric field has nodes at the interfaces and the displacement associated with the nth mode is[19]

$$u_{n+}=\cos(n\pi z/L)\ ,\quad n=1,3,5,\ldots, \tag{6}$$

$$u_{n-}=\sin(n\pi z/L)\ ,\quad n=2,4,6,\ldots\ . \tag{7}$$

Ridley's guided modes[20] are obtained by imposing boundary conditions only on atomic displacements at the interfaces. The model is based on hydrodynamic boundary conditions proposed by Babiker.[42] The displacement of the nth guided mode is

$$u_{n+}=\sin(n\pi z/L)\ ,\quad n=1,3,5,\ldots, \tag{8}$$

$$u_{n-}=\cos(n\pi z/L)\ ,\quad n=2,4,6,\ldots\ . \tag{9}$$

Finally, $t_{n\alpha}(q)$ is given by

$$t_{n\alpha}(q)=\left\{\frac{2}{L}\int_{-L/2}^{L/2}dz\left[q^2u_{n\alpha}^2+\left[\frac{du_{n\alpha}}{dz}\right]^2\right]\right\}^{-1/2}\ . \tag{10}$$

The evaluation of the integral gives

$$t_{n-}(q)=\left[3q^2+\frac{n^2\pi^2}{L^2}\right]^{-1/2}\ ,\quad n=2,4,6,\ldots, \tag{11}$$

and

$$t_{n+}(q)=\left\{\left[1+C_n^2\left[\frac{1}{6}-\mu_n^{-2}\pi^{-2}\right]\right]q^2+(\mu_n^2\pi^2-C_n^2)L^{-2}\right\}^{-1/2}\ ,\quad n=3,5,7,\ldots, \tag{12}$$

for the HZ model, and

$$t_{n\alpha}(q)=\left[q^2+\frac{n^2\pi^2}{L^2}\right]^{-1/2}\ ,\quad n=1,2,3,\ldots, \tag{13}$$

for the other two models.

B. Electron–interface-optical-phonon interaction

The Hamiltonian for electron–interface-optical-phonon interaction in a QW structure is given by[32]

$$H_\beta=\sum_{q,\mu}\left[\frac{2\pi e^2 f_{\beta\mu}}{\hbar A q\omega_{\beta\mu}}\right]^{1/2}\exp(i\mathbf{q}\cdot\mathbf{r})\left[\frac{\gamma}{1\pm\gamma}\right]^{1/2}\times\left[\exp(qz)\pm\exp(-qz)\right](a_{\beta\mu}(\mathbf{q})+a^\dagger_{\beta\mu}(-\mathbf{q}))\ , \tag{14}$$

where $a_{\beta\mu}, a^\dagger_{\beta\mu}$ are, respectively, the phonon annihilation and creation operators and A is the normalization area. The subscript β represents the symmetric (s) or antisymmetric (a) forms of the interface phonon modes and $\mu=\pm$ distinguishes the two interface phonon modes corresponding to the well ($-$) and the barrier ($+$) materials. In Eq. (14) the other quantities are

$$\gamma=\exp(-qL)\ , \tag{15}$$

$$f_{\beta\mu}=\left|\frac{\hbar^2(\omega^2_{\beta\mu}-\omega^2_{\mathrm{TO1}})(\omega^2_{\beta\mu}-\omega^2_{\mathrm{TO2}})}{(\omega^2_{\beta+}-\omega^2_{\beta-})(\varepsilon_{1\beta}+\varepsilon_{2\beta})}\right|\ , \tag{16}$$

$$\varepsilon_{1s}=\varepsilon_{1\infty}(1-\gamma)\ ,\quad \varepsilon_{1a}=\varepsilon_{1\infty}(1+\gamma)\ ,$$
$$\varepsilon_{2s}=\varepsilon_{2\infty}(1+\gamma)\ ,\quad \varepsilon_{2a}=\varepsilon_{2\infty}(1-\gamma)\ . \tag{17}$$

The index 1 refers to the well material (GaAs) and 2 to the barrier material (AlAs). ω_{TO1} and ω_{TO2} are the bulk TO-phonon frequencies, assumed to be dispersionless. $\varepsilon_{1\infty}$ and $\varepsilon_{2\infty}$ are the high-frequency dielectric constants of the well and barrier materials, respectively. The interface optical-phonon frequencies are given by

$$\omega^2_{\beta\mu}=\frac{\zeta\pm[\zeta^2-\hbar^4(\varepsilon_{1\beta}+\varepsilon_{2\beta})(\varepsilon_{1\beta}\omega^2_{\mathrm{LO1}}\omega^2_{\mathrm{TO2}}-\varepsilon_{2\beta}\omega^2_{\mathrm{LO2}}\omega^2_{\mathrm{TO1}})]^{1/2}}{(\varepsilon_{1\beta}+\varepsilon_{2\beta})\hbar^2}\ , \tag{18}$$

with

$$\zeta=\frac{\hbar^2}{2}[\varepsilon_{1\beta}(\omega^2_{\mathrm{TO2}}+\omega^2_{\mathrm{LO1}})+\varepsilon_{2\beta}(\omega^2_{\mathrm{TO1}}+\omega^2_{\mathrm{LO2}})]\ , \tag{19}$$

where ω_{LO1} and ω_{LO2} denote the bulk LO-phonon frequencies.

III. ABSORPTION COEFFICIENTS

The absorption coefficient can be related to the transition probabilities for the absorption and emission of photons. It can be expressed as[43]

$$K=\frac{\sqrt{\varepsilon}}{N_\nu c}\sum_i(W_i^{\mathrm{ab}}-W_i^{\mathrm{em}})f_i\ , \tag{20}$$

where ε is the dielectric constant of the medium, N_ν the number of photons in the radiation field, and f_i the electron distribution function. The sum is over all possible initial states i of the system. $W_i^{\mathrm{ab(em)}}$ is the transition probability for absorption (emission) of photons with simultaneous phonon absorption or emission.

The interaction Hamiltonian with radiation field is

$$H_{\mathrm{rad}}=-\frac{e}{m^*}\left[\frac{2\pi N_\nu\hbar}{\Omega\varepsilon V}\right]^{1/2}\mathbf{e}\cdot\mathbf{P}\ , \tag{21}$$

where $\mathbf{P}=\mathbf{p}-(e/c)\mathbf{A}_0$ is the generalized momentum in a static magnetic field with vector potential $\mathbf{A}_0=(0,Bx,0)$ and Ω the photon frequency. We consider a single-quantum-well structure where electrons are free to move in the x-y plane and a uniform static magnetic field $\mathbf{B}$ is applied in the z direction. Adopting a single-band spherical effective-mass model for electrons, the one-electron eigenfunctions Ψ_{Nlk_y} and energy eigenvalues E_{Nl} are given by

$$\Psi_{Nlk_y}=\left[\frac{1}{L_y}\right]^{1/2}\phi_N(x-x_0)\exp(ik_y y)\chi_l(z) \tag{22}$$

and

$$E_{Nl}=(N+1/2)\hbar\omega_c+l^2E_0\ , \tag{23}$$

where $N=0,1,2,\ldots$, $l=1,2,3,\ldots$, and $E_0=(\pi^2\hbar^2/2m^*L^2)$. ϕ_N represents the harmonic-oscillator wave function centered at $x_0=-\lambda^2k_y$ with $\lambda=(\hbar c/eB)^{1/2}$ being the cyclotron radius, and $\omega_c=|e|B/m^*c$ the cyclotron frequency. N denotes the Landau level index and l the electric subband quantum number. The envelope function is

$$\chi_l(z)=\left[\frac{2}{L}\right]^{1/2}\sin\left[\frac{l\pi z}{L}+\frac{l\pi}{2}\right]\ . \tag{24}$$

Using this wave function and assuming the electromagnetic field to be linearly polarized transverse to the magnetic field, the matrix elements for photon absorption can be written as

$$\langle N+1|H_{\mathrm{rad}}|N\rangle=\frac{e\hbar}{m^*}\left[\frac{2\pi N_\nu}{\hbar\Omega\varepsilon V}\right]^{1/2}\left[\frac{\hbar m^*\omega_c}{2}\right]^{1/2}\times(N+1)^{1/2}\ . \tag{25}$$

For the electron wave function given in Eq. (22) the matrix elements for the electron–confined-LO-phonon interaction can be expressed as

$$\langle k_y',N',l'|H_{\mathrm{el-ph}}|k_y,N,l\rangle=\left[\frac{4\pi e^2\hbar\omega_{\mathrm{LO1}}}{\varepsilon' V}\right]^{1/2}(N_{\mathrm{LO1}}+\tfrac{1}{2}\mp\tfrac{1}{2})^{1/2}\times t_{n\alpha}(q)J_{NN'}(u)G^{n\alpha}_{ll'}\delta_{k_y\pm q_y,k_y'}\ , \tag{26}$$

where N_{LO1} is the Bose distribution function characterized by phonon frequence ω_{LO1}, and

$$|J_{NN'}(u)|^2=\frac{n_2!}{n_1!}e^{-u}u^{n_1-n_2}[L^{n_1-n_2}_{n_2}(u)]^2\ , \tag{27}$$

with $u=\lambda^2q^2/2$, $n_1=\max(N,N')$, and $n_2=\min(N,N')$. $L^{n_1-n_2}_{n_2}$ are the associated Laguerre polynomials. $G^{n\alpha}_{ll'}$, is

given by

$$G_{ll'}^{n\alpha}=\int_{-L/2}^{L/2}\chi_{l'}(z)u_{n\alpha}(z)\chi_l(z)dz\ . \tag{28}$$

This overlap integral can easily be evaluated for intrasubband ($1\rightarrow 1$) and intersubband ($1\rightarrow 2$) transitions for all three models. In the HZ model only even modes and in slab modes only odd modes contribute for intrasubband transitions. For intersubband transitions, odd modes contribute in the HZ model and even modes in the slab model. In the case of guided modes, only the $n=2$ mode contributes for intrasubband transitions and the $n=1$ and 3 modes contribute for intersubband transitions.

For a nondegenerate Q2D electron gas in a quantizing magnetic field, the distribution function f_{Nl} can be shown to be

$$f_{Nl}=\frac{n_e\pi\lambda^2 L}{\xi}\exp\left[-\frac{l^2E_0}{k_BT}\right]\exp\left[-\frac{(N+\frac{1}{2})\hbar\omega_c}{k_BT}\right], \tag{29}$$

with

$$\xi=\sum_{l=1}\sum_{N=0}\exp\left[-\frac{(N+\frac{1}{2})\hbar\omega_c+l^2E_0}{k_BT}\right] \tag{30}$$

and n_e denoting the carrier concentration.

Using Eq. (20) and a straightforward calculation of transition probabilities, and replacing Dirac δ functions by a Lorentzian of width Γ, we obtain the following expression for the absorption coefficient for PACR in a nondegenerate Q2D electron system in a QW structure due to confined modes described by the HZ model:

$$K_{\rm CP}(B)=CA(\Omega,\omega_c)\left[\frac{\omega_{\rm LO1}}{\omega_c}\right]\sum_{N,N'}\sum_n\exp\left[-\frac{E_{1N}}{k_BT}\right]|G_{11}^{n-}|^2$$
$$\times\int_0^\infty dt\,t^3(3t^2+n^2\pi^2)^{-1}|J_{NN'}(t)|^2\Gamma'$$
$$\times\left\{\frac{N_{\rm LO1}}{\left[N'-N-\frac{\Omega}{\omega_c}-\frac{\omega_{\rm LO1}}{\omega_c}\right]^2+\Gamma'^2}+\frac{N_{\rm LO1}+1}{\left[N'-N-\frac{\Omega}{\omega_c}+\frac{\omega_{\rm LO1}}{\omega_c}\right]^2+\Gamma'^2}\right\}, \tag{31}$$

where $t=qL$,

$$E_{1N}=(N+1/2)\hbar\omega_c+E_0\ ,$$

$$C=\frac{\pi n_e e^4\lambda^2}{cm^*\varepsilon'\sqrt{\varepsilon}L^3\xi\omega_c\hbar\Omega}\ ,$$

$$A(\Omega,\omega_c)=\left[1+\frac{\Omega}{\omega_c}\right]^{-2}+\left[1-\frac{\Omega}{\omega_c}\right]^{-2},$$

$$G_{11}^{n-}=\tfrac{3}{2}\delta_{n,2}-(-1)^{n/2}(1-\delta_{n,2})\ ,$$

and $\Gamma'=\Gamma/\hbar\omega_c$. The subscript CP refers to confined phonons. The absorption coefficients for various models can be obtained by substituting appropriate $G_{ll'}^{n\alpha}$, and $T_{n\alpha}$.

The matrix element for electron–interface-phonon interaction is given by[44]

$$\langle k_y',N',l'|H_\beta|k_y,N,l\rangle=\left[\frac{2\pi e^2 f_{\beta\mu}}{\hbar Aq\omega_{\beta\mu}}\right]^{1/2}\left[\frac{\gamma}{1\pm\gamma}\right]^{1/2}$$
$$\times(N_{\beta\mu}+\tfrac{1}{2}\mp\tfrac{1}{2})^{1/2}G_{ll'}^{\beta}J_{NN'}(u)$$
$$\times\delta_{k_y\pm q_y,k_y'}\ , \tag{32}$$

where

$$N_{\beta\mu}=\left[\exp\left[\frac{\hbar\omega_{\beta\mu}}{k_BT}\right]-1\right]^{-1}$$

is the Bose distribution function for the interface mode, the function $J_{NN'}(u)$ is as defined in Eq. (27), and $G_{ll'}^{\beta}$ are now given by

$$G_{ll'}^{\beta}=\int_{-L/2}^{L/2}dz\,\chi_{l'}^*(z)[\exp(qz)\pm\exp(-qz)]\chi_l(z)\ . \tag{33}$$

The evaluation of this integral is given in Ref. 44 [Eqs. (14)–(17)], and for intrasubband transitions ($1\rightarrow 1$) only the symmetric modes contribute.

Using Eq. (20) and a straightforward calculation of transition probabilities, the absorption coefficient for PACR due to interface optical phonons becomes

$$K_{\rm IP}(B)=C_{\rm IP}A(\Omega,\omega_c)\sum_{N,N',\mu}\exp\left[-\frac{E_{1N}}{k_BT}\right]\int_0^\infty dt\,t^2e^{-t}(1+e^{-t})^{-1}|G_{11}^{s}|^2|J_{NN'}(t)|^2\left[\frac{f_{s\mu}}{\hbar^2\omega_c\omega_{s\mu}}\right]\Gamma'$$
$$\times\left\{\frac{N_{s\mu}}{\left[N'-N-\frac{\Omega}{\omega_c}-\frac{\omega_{s\mu}}{\omega_c}\right]^2+\Gamma'^2}+\frac{N_{s\mu}+1}{\left[N'-N-\frac{\Omega}{\omega_c}+\frac{\omega_{s\mu}}{\omega_c}\right]^2+\Gamma'^2}\right\}, \tag{34}$$

with

$$C_{\mathrm{IP}}=\frac{\pi e^4\lambda^2 n_e}{2cm^*\sqrt{\varepsilon}L^3\hbar\Omega\omega_c}\ ,$$

and

$$G_{11}^s=\frac{8\pi^2}{t}\exp\left[\frac{t}{2}\right](1-\gamma)(t^2+4\pi^2)^{-1}\ .$$

The subscript IP refers to interface phonons. Equations (31) and (34) can be compared with the following expression for the PACR absorption coefficient which we have obtained for the bulk description of phonons in a QW structure:

$$K_{\mathrm{BP}}(B)=\frac{C}{2}\left[\frac{\omega_{\mathrm{LO1}}}{\omega_c}\right]A(\Omega,\omega_c)\sum_{N,N'}\exp\left[-\frac{E_{1N}}{k_BT}\right]$$
$$\times\int_0^\infty dt\,t^3|J_{NN'}(t)|^2\left\{t^{-2}[1-F(t)]+\left[0.5+\left[2-\frac{t^2}{t^2+4\pi^2}\right]F(t)\right](t^2+4\pi^2)^{-1}\right\}$$
$$\times\Gamma'\left\{\frac{N_{\mathrm{LO1}}}{\left[N'-N-\frac{\Omega}{\omega_c}-\frac{\omega_{\mathrm{LO1}}}{\omega_c}\right]^2+\Gamma'^2}+\frac{N_{\mathrm{LO1}}+1}{\left[N'-N-\frac{\Omega}{\omega_c}+\frac{\omega_{\mathrm{LO1}}}{\omega_c}\right]^2+\Gamma'^2}\right\}, \tag{35}$$

where $F(t)=(1-e^{-t})/t$. The subscript BP refers to bulk phonons.

IV. RESULTS AND DISCUSSION

We have evaluated numerically the above expressions for absorption coefficients obtained for electron interaction with confined, interface, and bulk phonons in the GaAs/AlAs QW system. The material parameters used are[45] $\hbar\omega_{\mathrm{LO1}}=36.2$ meV, $\hbar\omega_{\mathrm{LO2}}=50.09$ meV, $\hbar\omega_{\mathrm{TO1}}=33.29$ meV, $\hbar\omega_{\mathrm{TO2}}=44.28$ meV, $\varepsilon_{1\infty}=10.89$, $\varepsilon_{2\infty}=8.16$, and $m^*=0.067m_0$. Figure 1 shows the variation of absorption coefficient with Ω/ω_c, for bulk phonons (full curve), confined phonons described by the HZ model (dashed curve), symmetric interface AlAs-like (ω_{s+}) modes (dot-dashed curve), and symmetric interface GaAs-like (ω_{s-}) modes (dotted curve), calculated for a QW of width $L=100$ Å at $T=77$ K, $B=10$ T. The surface concentration of electrons n_s ($=n_eL$) is taken to be 1.0×10^{11} cm^{-2}. The Landau level width Γ is assumed to be 1 meV. This value of the broadening parameter is reasonable, according to the results of our recent self-consistent calculations of electron scattering rates in GaAs/AlAs QW's due to confined[27] and interface[44] phonons in the presence of a quantizing magnetic field. The main cyclotron resonance occurs at $\Omega=\omega_c$. The singularity at $\Omega=\omega_c$ in the figure is associated with the factor $A(\Omega,\omega_c)$ in Eqs. (31), (34), and (35). The other peaks in the curves correspond to the phonon-assisted resonance transitions between the Landau levels. These transitions can be of different types depending upon the Landau level separation and photon and phonon energies. Possible processes are shown in Figs. 2–4. Figure 2 is for the case $\omega_c>\omega_p$, where ω_p represents the phonon frequency. In this case absorption of a photon is possible only by a transition to a higher Landau level. Further, different

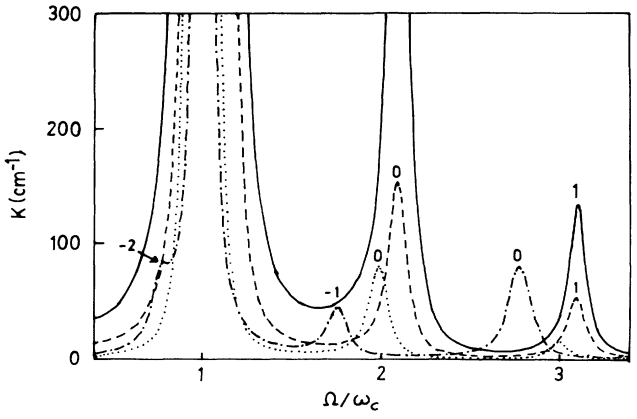

FIG. 1. Dependence of the absorption coefficient on Ω/ω_c calculated for $L=100$ Å at $T=77$ K and $B=10$ T. The full curve is for bulk phonons, the dashed curve is for confined modes described by the HZ model, the dot-dashed curve is for interface ω_{s+} modes, and the dotted curve is for interface ω_{s-} modes.

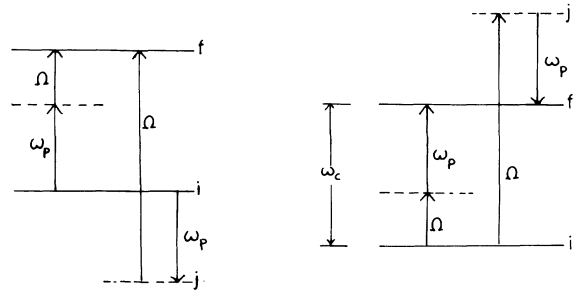

FIG. 2. PACR transitions that lead to resonance when ω_c is larger than the optical-phonon frequency ω_p.

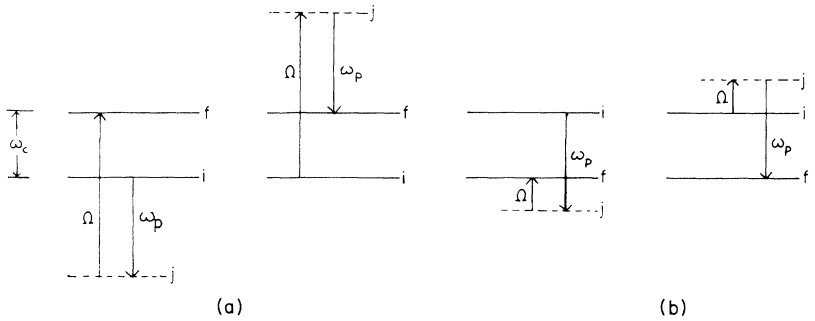

FIG. 3. PACR transitions which lead to resonance when ω_c is smaller than ω_p (a) for $\Omega > \omega_p$ and (b) for $\Omega < \omega_p$.

possibilities like $\Omega > \omega_p$ and $\Omega < \omega_p$ are also shown. In the figures, i, f, and j denote the initial, final, and intermediate levels, respectively. The resonance frequencies are given by $\Omega = \omega_c \mp \omega_p$. The upper sign $(-)$ and the lower sign $(+)$ correspond, respectively, to phonon absorption and emission. The transitions for $\omega_c < \omega_p$ can be of four different types as shown in Fig. 3. In this case only transitions with phonon emission are possible. Figure 3(a) shows the case in which $\Omega > \omega_p$ and the transitions cause resonance at $\Omega = \omega_p + \omega_c$. Figure 3(b) shows the case in which $\Omega < \omega_p$ and the transitions cause resonance at $\Omega = \omega_p - \omega_c$. The transitions which lead to resonance absorption when electrons remain in the same Landau level are shown in Fig. 4. The intermediate level can be an upper or lower level and $\Omega = \omega_p$. These phonon-assisted transitions are not restricted only to the neighboring Landau levels. Electrons can undergo resonant transitions between Landau levels with energy separation $m\hbar\omega_c$, with m being an integer. Thus conditions for resonant transitions, in general, can be written as $\Omega = \omega_p + m\omega_c$ for the cases shown in Fig. 3. Resonant transitions are also possible when $\Omega = \omega_p = m\omega_c$.

For a magnetic field of strength $B = 10$ T, the energy separation of the Landau levels is smaller than the phonon energy, and peaks other than that at $\Omega = \omega_c$ in Fig. 1 are due to the transitions shown in Figs. 3 and 4. It may be noted that peaks due to confined phonon modes coincide with those of bulk phonons. This is due to equivalence in the energies of bulk and confined phonons. However, the magnitude of the absorption coefficient due to confined phonons is lower than that due to bulk phonons. The peak value of K_{CP} corresponding to $m = 1$ is 40.7% of that due to bulk phonons. In the HZ model only even modes contribute and the maximum contribution is from $n = 2$, whereas in the case of bulk phonons all modes contribute. The resonance peaks due to confined modes described by the slab and guided mode models occur at the same positions as those for the bulk phonons. The peaks due to confined and bulk phonons occurring at $\Omega/\omega_c = 2.09$ are due to transitions of the type shown in Fig. 4, and the value of m is taken as zero as the electron remains in the initial Landau level at the end of the process. The peaks at $\Omega/\omega_c = 3.1$ are due to transitions of the type shown in Fig. 3(a) and the value of m is 1. The numbers on the top of the peaks in Fig. 1 indicate the value of m.

The interface modes ω_{s+} and ω_{s-} are dispersive in nature and we have taken this into consideration in our calculations. The range of dispersion for the ω_{s+} mode is from 47.42 to 50.09 meV and for the ω_{s-} mode from 33.29 to 34.64 meV. The resonance peaks due to these modes are found to occur at the average values of the respective limits of dispersion. The peak at $\Omega/\omega_c = 1.76$ is for the ω_{s+} mode and is due to a transition of the type shown in Fig. 3(a) with $m = -1$. A kink in the left-hand side of the main cyclotron resonance singularity is due to a similar transition but for $m = -2$. The peak at $\Omega/\omega_c = 2.78$ is due to a transition of the type shown in Fig. 4 and the photon energy corresponding to this is 48.16 meV, which is the average of the range of disper-

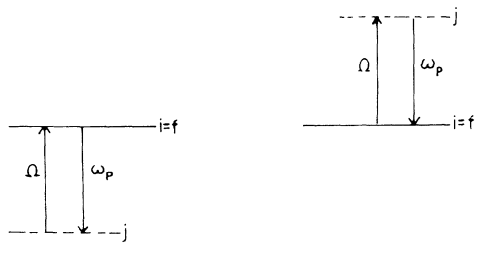

FIG. 4. PACR transitions leading to resonant absorption when electrons remain in the initial Landau level.

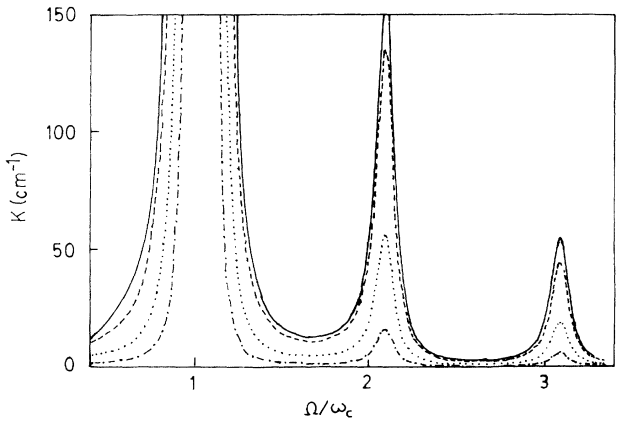

FIG. 5. PACR absorption spectrum shown as a function of Ω/ω_c due to confined modes described by the HZ model (full curve), slab modes (dashed curve), and guided modes (dot-dashed curve), calculated for $L = 100$ Å, $B = 10$ T, and $T = 77$ K. The dotted curve is due to the HZ model for a QW with finite barrier height of 1 eV.

sion of the ω_{s+} mode. In the measurements of *I-V* characteristics of phonon-assisted tunneling in GaAs/$Ga_{1-x}Al_xAs$ double-barrier tunneling structures Leadbeater *et al.*[15] have estimated the energy of the interface AlAs-like mode to be 48.5 meV. The resonance peaks for ω_{s-} modes occur at $\Omega/\omega_c = 1.99$ and 2.98 and are due to transitions of the type shown in Figs. 4 and 3(a), respectively. The corresponding values of m are 0 and 1. The magnitude of the absorption coefficient due to interface modes is smaller than that due to confined and bulk phonons. This indicates weak coupling between electrons and the interface phonon modes at large well widths.

Figure 5 shows the absorption spectrum due to confined phonons described by the HZ model (full curve), slab model (dashed curve), and guided mode model (dot-dashed curve). Resonant peak positions coincide in all the three models. The magnitudes of the peak value corresponding to $m=1$ due to slab and guided modes are, respectively, 82.5% and 10.9% of that obtained with the HZ model. The large difference in the case of guided modes is due to the involvement of only the $n=2$ mode in the phonon-assisted transitions. The dotted curve in the figure is for the HZ model calculated with a finite height of 1 eV for the QW barrier. The effect of the finite depth for the QW is to reduce the absorption coefficient.

The variation of the sum of the absorption coefficients due to confined modes described by the HZ model and the interface (ω_{s+} and ω_{s-}) modes with Ω/ω_c is shown in Fig. 6. For the sake of comparison we have drawn the figure to the scale of Fig. 1. The resonance peaks due to interface ω_{s+} modes appear as satellite peaks to the peaks due to the confined modes and are strong enough to be detected in a PACR experiment.

The dependence of absorption coefficient on well width is shown in Fig. 7 calculated at $T=77$ K, $B=10$ T, and $m=1$. Curve 1 is for bulk phonons, 2 for confined, 3 for the ω_{s+} mode, and 4 for the ω_{s-} mode. It can be noted that for well widths less than 70 Å electron interaction with interface modes dominates over that with confined modes. However, the absorption coefficient, in general, decreases with increasing well width.

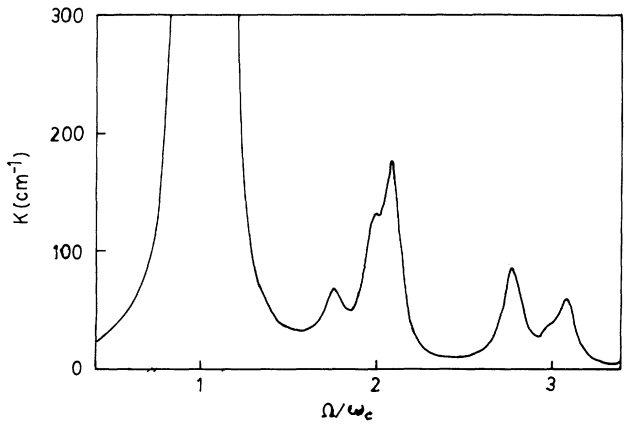

FIG. 6. Sum of absorption coefficients due to confined modes described by the HZ model and interface modes ω_{s+} and ω_{s-} shown as a function of Ω/ω_c.

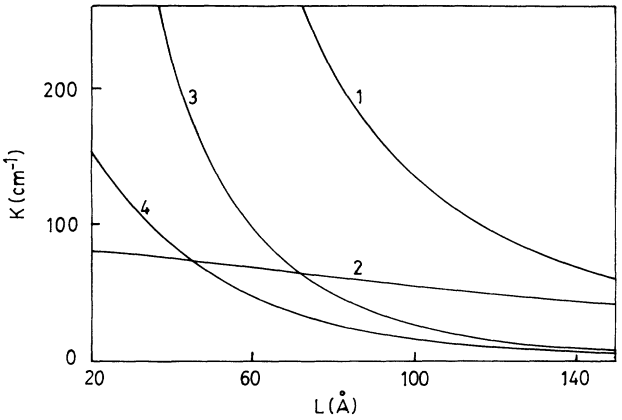

FIG. 7. Well-width dependence of the peak value of the absorption coefficients for $\Omega=\omega_c+\omega_p$ ($m=1$) due to bulk phonons (curve 1), confined modes described by the HZ model (curve 2), interface ω_{s+} modes (curve 3), and interface ω_{s-} modes (curve 4), calculated at $B=10$ T, $T=77$ K.

Figure 8 displays the magnetic-field dependence of the peak value of the absorption coefficients calculated for $L=100$ Å and $m=1$. Curve 1 is for bulk phonons, 2 for confined phonons, 3 for ω_{s+} modes, and 4 for ω_{s-} modes. The absorption coefficients due to bulk and confined phonons increase with increasing magnetic field whereas that due to interface modes become saturated at large magnetic fields.

We have also investigated the dependence of the absorption coefficients due to confined and interface phonon modes on the broadening parameter Γ for $B=10$ T and $L=100$ Å. The height and the sharpness of the peaks in the absorption spectrum decrease with increase of Γ. Our results for the overall behavior of the absorption coefficient with well width, magnetic field, and broadening parameter are in agreement with the calculations of

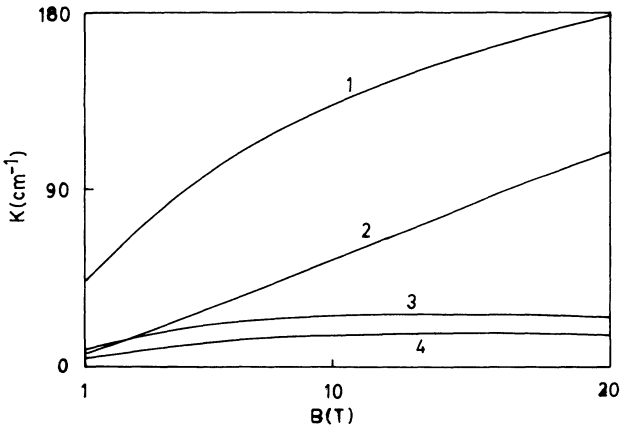

FIG. 8. Field dependence of the peak value of absorption coefficients for $\Omega=\omega_c+\omega_p$ ($m=1$) calculated for a QW of width $L=100$ Å at $T=77$ K. Curve 1 is for bulk phonons, 2 for confined phonons (HZ model), 3 for interface ω_{s+} modes, and 4 for interface ω_{s-} modes.

Hai, Peeters, and Devreese.[39]

In conclusion, we have presented a theory of PACR in Q2D semiconducting quantum-well structures using a perturbation technique, when electrons are scattered by confined and interface optical phonons. Additional peaks in the absorption spectrum due to interface-phonon-assisted transitions, apart from those due to confined phonons, are predicted. It would be interesting to have experimental results to test the predictions of the present calculations. The peaks due to interface modes are strong enough to be detected.

ACKNOWLEDGMENTS

The author J.S.B. is thankful to the management of S. D. M. College of Engineering for encouragement. One of us (B.G.M.) is grateful to ICTP, Trieste, Italy for their hospitality. This work was supported by UGC India.

*Author to whom all correspondence should be addressed.

[1]T. Ando, A. B. Fowler, and F. Stern, Rev. Mod. Phys. **54**, 437 (1982).

[2]J. T. Devreese and F. M. Peeters, in *The Physics of Two Dimensional Electron Gas*, edited by J. T. Devreese and F. M. Peeters (Plenum, New York, 1987).

[3]F. G. Bass and I. B. Levinson, Zh. Eksp. Teor. Fiz. **49**, 914 (1965) [Sov. Phys. JETP **22**, 635 (1966)].

[4]R. K. Bakanas, Fiz. Tverd. Tela (Leningrad) **12**, 3408 (1971) [Sov. Phys. Solid State **12**, 2769 (1971)].

[5]T. M. Rynne and H. N. Spector, J. Appl. Phys. **52**, 393 (1981).

[6]M. W. Goodwin and D. G. Seiler, Phys. Rev. B **27**, 3451 (1983).

[7]R. C. Enck, A. S. Saleh, and H. Y. Fan, Phys. Rev. **182**, 790, (1969).

[8]E. J. Johnson and D. H. Dickey, Phys. Rev. B **1**, 2676 (1970).

[9]M. Singh and B. Tanatar, Phys. Rev. B **41**, 12 781 (1990).

[10]B. Tanatar and M. Singh, Phys. Rev. B **42**, 3077 (1990).

[11]J. S. Bhat, S. S. Kubakaddi, and B. G. Mulimani, J. Appl. Phys. **70**, 2216 (1991).

[12]B. Jusserand and M. Cardona, in *Light Scattering in Solids V*, edited by M. Cardona and G. Güntherodt (Springer, Heidelberg, 1989).

[13]M. V. Klein, IEEE J. Quantum Electron. **QE-22**, 1760 (1986).

[14]J. Menendez, J. Lumin. **44**, 285 (1985).

[15]M. L. Leadbeater, E. S. Alves, L. Eaves, M. Henini, O. H. Hughes, A. Celeste, J. C. Portal, G. Hill, and M. A. Pate, Phys. Rev. B **39**, 3438 (1989).

[16]J. G. Chen, C. H. Yang, M. J. Yang, and R. A. Wilson, Phys. Rev. B **43**, 4531 (1991).

[17]P. J. Turley and S. W. Teitsworth, Phys. Rev. B **44**, 12 959 (1991).

[18]R. Fuchs and K. L. Kliewer, Phys. Rev. **140**, A2076 (1965).

[19]J. J. Licari and R. Evrard, Phys. Rev. B **15**, 2254 (1977).

[20]B. K. Ridley, Phys. Rev. B **39**, 5282 (1989).

[21]K. Huang and B. Zhu, Phys. Rev. B **38**, 2183 (1988); **38**, 13 377 (1988).

[22]S. Rudin and T. L. Reinecke, Phys. Rev. B **41**, 7713 (1990); **43**, 9298 (1991).

[23]G. Weber, A. M. de Paula, and J. F. Ryan, Semicond. Sci. Technol. **6**, 397 (1991).

[24]M. C. Tatham, J. F. Ryan, and C. T. Foxon, Phys. Rev. Lett. **63**, 1637 (1989).

[25]A. Seilmeier, H.-J. Hübner, G. Abstreiter, G. Weimann, and W. Schlapp, Phys. Rev. Lett. **59**, 1345 (1987).

[26]G. Weber and J. F. Ryan, Phys. Rev. B **45**, 11 202 (1992).

[27]J. S. Bhat, B. G. Mulimani, and S. S. Kubakiddi, Semicond. Sci. Technol. **8**, 1571 (1993).

[28]I. C. da Cunha Lima and T. L. Reinecke, Phys. Rev. B **46**, 1620 (1992).

[29]J. S. Bhat, B. G. Mulimani, and S. S. Kubakaddi, J. Appl. Phys. **72**, 4966 (1992).

[30]K. T. Tsen, K. R. Wald, T. Ruf, P. Y. Yu, and H. Morkoç, Phys. Rev. Lett. **67**, 2557 (1991).

[31]T. Ruf, K. Wald, P. Y. Yu, K. T. Tsen, H. Morkoç, and K. T. Chang, Superlatt. Microstruct. **13**, 203 (1993).

[32]R. Lassnig, Phys. Rev. B **30**, 7132 (1984).

[33]L. Wendler, Phys. Status Solidi B **129**, 513 (1985).

[34]L. Wendler and R. Pechstedt, Phys. Status Solidi B **141**, 129 (1987).

[35]N. Mori and T. Ando, Phys. Rev. B **40**, 6175 (1989).

[36]R. Chen, D. L. Lin, and T. F. George, Phys. Rev. B **41**, 1435 (1990).

[37]G. Weber, Solid State Commun. **84**, 595 (1992); J. Phys. Condens. Matter **4**, 9831 (1992).

[38]A. J. Shields, C. Trallero-Giner, M. Cardona, H. T. Grahn, K. Ploog, V. A. Haisler, D. A. Tenne, N. T. Moshegov, and A. I. Toropov, Phys. Rev. B **46**, 6990 (1992).

[39]G. Q. Hai, F. M. Peeters, and J. T. Devreese, Phys. Rev. B **47**, 10 358 (1993).

[40]H. Adamska and H. N. Spector, J. Appl. Phys. **56**, 1123 (1984).

[41]S. S. Kubakaddi and B. G. Mulimani, J. Appl. Phys. **58**, 3640 (1985); J. Phys. C **18**, 6647 (1985).

[42]M. Babiker, J. Phys. C **19**, 683 (1986).

[43]H. Meyer, Phys. Rev. **112**, 298 (1958).

[44]J. S. Bhat, B. G. Mulimani, and S. S. Kubakaddi, J. Appl. Phys. **74**, 4561 (1993).

[45]S. Adachi, J. Appl. Phys. **58**, R1 (1985).